

X-ray standing wave imaging of the $\frac{1}{3}$ monolayer Sn/Ge(111) surface

J. S. Okasinski,¹ C.-Y. Kim,¹ D. A. Walko,^{1,*} and M. J. Bedzyk^{1,2}

¹Department of Materials Science and Engineering, Northwestern University, Evanston, Illinois 60208, USA

²Materials Research Center, Northwestern University, Evanston, Illinois 60208, USA

(Received 6 October 2003; published 8 January 2004)

X-ray standing waves (XSW) are used to measure the structure of the $(\sqrt{3}\times\sqrt{3})R30^\circ$ to (3×3) low-temperature phase transition for the $\frac{1}{3}$ monolayer Sn/Ge(111) surface. A three-dimensional direct-space imaging approach, based on the summation of several hkl XSW-measured Fourier coefficients, is demonstrated. At room temperature, the Sn atoms are found to occupy the T_4 -adsorption sites with one-third of the Sn atoms 0.45 Å higher than the remaining two-thirds. The (3×3) phase has no significant change in the XSW-measured structural parameters. This is consistent with an order-disorder-type phase transition.

DOI: 10.1103/PhysRevB.69.041401

PACS number(s): 68.35.Rh, 68.43.Fg, 68.49.Uv, 61.10.-i

Insight into the two-dimensional (2D) physics of surface phase transitions, dynamics, and kinetics often requires an accurate atomic-scale description. For example, at room temperature (RT), the $\frac{1}{3}$ ML (monolayer) Sn on Ge(111) surface forms a $(\sqrt{3}\times\sqrt{3})R30^\circ$ (to be called $\sqrt{3}$) reconstruction and is typically modeled with a single Sn atom occupying one of three T_4 -adsorption sites in the $\sqrt{3}$ unit cell (see Fig. 1).^{1,2} When cooling from the critical temperature ($T_C\sim 210$ K) to near 100 K, the surface reconstruction completes a gradual and reversible transition to a (3×3) phase.³ Scanning tunneling microscopy (STM) images show one of the T_4 -site Sn atomic protrusions in the (3×3) unit cell appearing different than the other two.³ Despite numerous investigations into this system, the structure and nature of this transition are still unresolved.⁴⁻¹³ To study this apparent broken symmetry in the atomic distribution, we have developed a method for 3D imaging of adsorbate atoms on crystalline surfaces that is based on the direct Fourier inversion of x-ray standing wave (XSW) data.

The leading models for this phase transition generally fall into either a displacive or an order-disorder transition. In the former, one model is that Ge atoms replace Sn atoms on the surface to form substitutional point defects.^{14,15} At RT the Sn atoms nearest to the Ge defects appear as small regions of (3×3) phase that increase in area as the temperature is lowered.¹⁵ Petersen *et al.*¹⁶ proposed that the Ge defects locally freeze in a soft phonon mode¹¹ for the (3×3) phase. In an order-disorder explanation of the transition, Avila *et al.*⁶ used molecular dynamics to show that the vertical distribution of Sn atoms is attributed to dynamical fluctuations where the Sn atoms fluctuate between the two heights and spend little time in transition between the two positions. At low temperature (LT), the three Sn atoms in the unit cell are locked into a “one up and two down” configuration with long-range order and form the ground-state (3×3) phase. As the temperature increases, the long-range order in the vertical distribution of the Sn atoms is lost because the Sn atoms undergo correlated, rapid fluctuations between the two heights. At RT STM and diffraction observe the smaller $\sqrt{3}$ unit cell because all of the Sn atoms appear equivalent due to time averaging of the rapid interchanging of their heights.

To better understand this phase transition, the atomic-scale structures for the phases need to be accurately quanti-

fied. Several surface x-ray-diffraction (SXRD) experiments have been completed for this system but have come to somewhat different conclusions.^{7,8,10} The main controversies are whether the Sn atoms (and underlying Ge atoms) possess a rippled topography at both RT and LT, and whether the topography is one up and two down or “two up and one down.”

Because the XSW is generated by dynamical Bragg diffraction from the bulk Ge crystal, it does not require long-range ordering of Sn atoms to sense their vertical distribution. XSW results are element specific, model-independent, and provide the projected positions of the Sn atoms within the 3D primitive unit cell of the bulk Ge crystal.¹⁷⁻²¹ With measurements at both RT and LT, the time-averaged vertical distributions for Sn can be compared. A model with displacement of Sn atoms would predict that the XSW results would differ between the RT and LT, while the XSW finding of an unchanged vertical distribution would support an order-disorder transition.

Typically, to determine the adsorption site with the XSW technique, the positions of the atoms are triangulated using two measurements, one normal and the other off-normal to

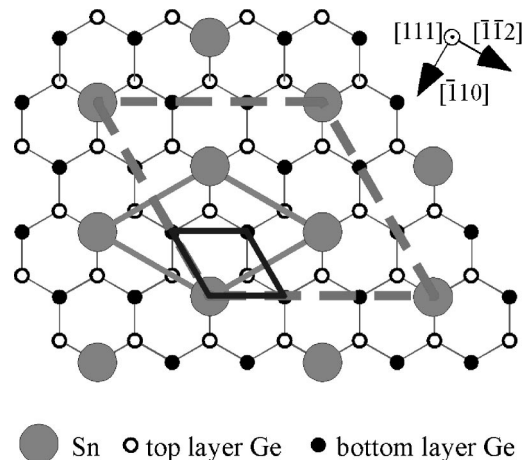


FIG. 1. Top view of the $\frac{1}{3}$ ML Sn/Ge(111) surface showing the top Ge bilayer (two layers separated by $d_{111}/4$) and Sn adatoms in one-third of the T_4 sites. The (1×1) , $\sqrt{3}$, and (3×3) surface unit cells are drawn in black, grey, and dashed lines, respectively.

the surface. In general and especially in cases of more than one adsorption site per unit cell, it is desirable to determine the position of atoms without assuming a model prior to the analysis. In this paper we present a XSW direct-space imaging procedure, which is a different approach for determining the locations of the adsorbates on crystalline surface. The first step in the analysis is to create an atomic-density map with low resolution (0.5 Å). The second stage uses conventional XSW analysis and a model based on the image to determine the Sn adatom position with high resolution (0.04 Å).

The sample preparation and measurements were performed in an ultrahigh-vacuum chamber coupled to a six-circle diffractometer located at the 5ID-C DND-CAT undulator station of the Advanced Photon Source.²² The base pressure for the chamber was 2×10^{-10} torr. The Ge(111) surface was argon-ion sputter cleaned and annealed until low-energy electron diffraction (LEED) showed a well-ordered $c(2 \times 8)$ reconstruction. Sn was evaporated onto the clean surface at RT, and the sample was annealed to 473 K to obtain a sharp $\sqrt{3}$ LEED pattern. Upon cooling the sample to 115 K, the surface displayed a (3×3) reconstruction. The coverage of Sn on the surface was determined to be 0.29(3) ML by *ex situ* Rutherford backscattering spectroscopy.

During the XSW measurements, the Ge single-crystal substrate was scanned in angle through a selected hkl Bragg peak, and the induced modulation in the Sn L x-ray fluorescence yield was measured using a solid-state Ge detector. The incident-beam energy was set at $E_\gamma = 7.00$ keV by the Si(111) high-heat-load 5ID monochromator and horizontally focused with a pair of glass mirrors. The beam was further conditioned with a pair of nondispersive, Si channel-cut (two-bounce) postmonochromators that were tuned to produce a strongly modulating XSW in Ge. For each hkl reflection from the Ge substrate, the corresponding hkl reflection was selected for the Si postmonochromators to minimize dispersion. Two Bragg reflections normal to the surface, (111) and (333), and two off-normal reflections, $(11\bar{1})$ and $(33\bar{3})$, were measured at RT and LT.

Conventional x-ray-diffraction methods suffer from the so-called “phase problem” because only the amplitude of the diffracted plane wave is detected. Whereas in XSW, the “detector” is the fluorescent atom, located within the interference field, which senses both the amplitude and the phase of the diffracted plane wave. For this reason, the XSW technique determines the amplitudes f_H as well as the phases P_H of the measured Fourier coefficients, $F_H = f_H \exp(2\pi i P_H)$. In the formalism of crystallography, these are the geometrical structure factors (including the Debye-Waller factor) for the individual sublattices of each fluorescent atomic species. Dynamical diffraction theory was used to fit the reflectivity (rocking) curve $R(\theta)$, and the fluorescence yield $Y(\theta)$, to obtain the coherent position P_H and coherent fraction f_H for the Sn atoms.^{20,21} In the dipole approximation for the photoelectric effect, the normalized XSW fluorescence yield for an adatom is

$$Y(\theta) = 1 + R(\theta) + 2 f_H \sqrt{R(\theta)} \cos(\nu(\theta) - 2\pi P_H). \quad (1)$$

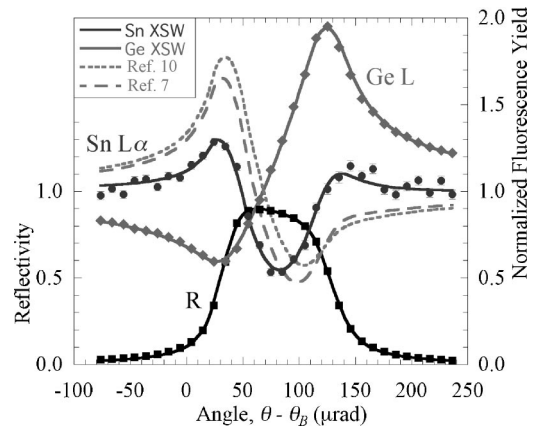


FIG. 2. RT (111) XSW results showing the angular dependence of the experimental and theoretical curves for reflectivity and fluorescent yields for Sn $L\alpha$ and Ge L . For comparison, the predicted yield curves based on the SXR models (Refs. 7 and 10) are shown.

The 180° phase shift in the XSW phase, $\nu(\theta)$, while scanning in angle θ through the Bragg peak causes a modulation in the yield that is sensitive to the atomic positions. To verify that the data collection and analysis procedure were responding correctly, the Ge L x-ray fluorescence from the substrate was analyzed and found to agree with the Ge bulk crystal structural positions ($P_{111} = 0.88, f_{111} = 0.70$). The (111) RT results are shown in Fig. 2 as a representative set of XSW data and analysis. In this analysis the origin is centered on the ideal bulklike Ge site in the top of the bilayer. The XSW results for this sample are summarized in Table I. At both 300 K and 115 K the measured P_H are the same, within experimental error. The reduction in f_H at LT is caused by Sn interacting over time with adsorbed gases. During the XSW experiments, the normal (111) reflection was measured several times to monitor the decrease of f_{111} (P_{111} remained constant). The fraction of randomly distributed Sn ($1-C$) increased by 10% over a 24 h period. Just before and after cooling the sample to 115 K, identical results were obtained for P_{111} and f_{111} at both RT and LT. In general, f_H decreases with C as the separation between atoms approaches $d_{hkl}/2$.

Generating a direct-space atomic-density map $\rho(r)$ from XSW-measured Fourier coefficients is simple and straightforward. One needs only to accurately measure a set of Fou-

TABLE I. Summary of the XSW results for a 0.29(3) ML Sn/Ge(111) surface. The origin ($P_H = 0$) is centered on the bulklike Ge site in the top of the bilayer.

hkl	$T = 300$ K		$T = 115$ K	
	P_H	f_H	P_H	f_H
(111)	0.63(1)	0.73(1)	0.64(1)	0.63(1)
$(11\bar{1})$	0.54(2)	0.75(2)	0.53(2)	0.64(2)
(333)	0.77(2)	0.33(2)	0.82(3)	0.22(3)
$(33\bar{3})$	0.62(2)	0.52(2)		

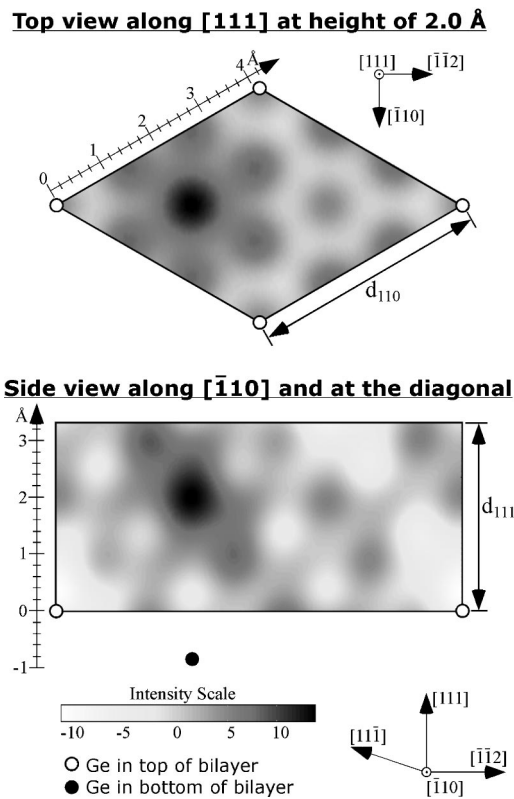


FIG. 3. XSW direct-space atomic-density maps for the $\frac{1}{3}$ ML Sn/Ge(111) surface at RT. The XSW measurements project the extended structure into the primitive unit cell of the bulk crystal. The top view corresponds to the (1×1) 2D unit cell shown in Fig. 1. The circles added to the image represent the top bilayer bulklike Ge atomic sites.

rier coefficients over a sufficient range of reciprocal space, apply certain symmetry rules,²³ and sum up the Fourier terms:²⁴

$$\begin{aligned} \rho(\mathbf{r}) &= \sum_{\mathbf{H}} \mathbf{F}_{\mathbf{H}} \exp[-2\pi i(\mathbf{H} \cdot \mathbf{r})] \\ &= 1 + 2 \sum_{\mathbf{H} \neq -\mathbf{H} \neq 0} f_{\mathbf{H}} \cos[2\pi(\mathbf{P}_{\mathbf{H}} - \mathbf{H} \cdot \mathbf{r})]. \end{aligned} \quad (2)$$

Inserting the RT XSW-measured amplitudes and phases of Table I into Eq. (2) produces the direct-space images shown in Fig. 3. The top view is a cross-sectional cut through the 3D image at 2.0 \AA above the surface, and the side view is through the long diagonal of the (1×1) unit cell. In these images the dark spots, representing the Sn atom maximum density, are located in the T_4 -adsorption site and are centered $\sim 2.0 \text{ \AA}$ above the top of the bulklike bilayer. In addition to this evidence from the XSW image, the T_4 -adsorption site is confirmed by the XSW measurements obeying the crystallographic symmetry relationship $P_{11\bar{1}} = (P_{111} + 1)/3$. The density oscillations appearing in the image are the result of unmeasured Fourier coefficients that abruptly truncate the summation. Since the XSW is generated by the Ge substrate, the atomic distribution is projected into the primitive unit

cell of the Ge crystal. Thus if there are two distinct heights in the 2D superlattice, their projections will superimpose to form a combined distribution. The resolution of this method along the $[111]$ direction corresponds to one-half of the smallest d spacing measured, in this case $d_{333}/2 = 0.5 \text{ \AA}$. Within this resolution, the Sn distribution is elongated in the $[111]$ direction, but does not show two distinct positions in the direct-space image. Rather, the two positions are smeared together and result in a bottom-heavy ovoid shape in the direction normal to the surface.

While the XSW direct-space imaging technique is useful for determining the position of the adsorbate *a priori*, the XSW results can also be used to precisely determine the positions of the Sn atoms with respect to a model that is suggested by this XSW direct-space image and other techniques. Using the normal (111) and (333) XSW measurements, the vertical distribution for the Sn atoms can be determined using a model with the following constraints: (1) a fraction C of Sn atoms are at T_4 sites; (2) the remaining fraction $(1-C)$ are randomly distributed; (3) for Sn at the T_4 sites, $\frac{1}{3}$ are at height h_A and $\frac{2}{3}$ are at height h_B ; (4) the rms vibrational amplitudes $\langle u^2 \rangle^{1/2}$ for all Sn atoms are identical and isotropic. The $\frac{1}{3}$ and $\frac{2}{3}$ weightings are based on the 1:2 Sn arrangement observed with STM at LT.³

These model constraints permit a single absorption height and do not necessarily assume a one up and two down, or two up and one down, configuration. The fact that P_{333} is measured to be less than $3P_{111} \text{ modulo } 1$ (i.e., $0.77 < 0.89$) indicates a bottom-heavy, asymmetric distribution that is consistent with one up and two down. If the time-averaged up-to-down occupation ratio were even, P_{333} would equal $3P_{111} \text{ modulo } 1$; and if it were 2:1, P_{333} would be greater than $3P_{111} \text{ modulo } 1$. A Fourier coefficient in the $[111]$ direction and its measured amplitude f_H and measured phase P_H are related to the four parameters of the model as follows:

$$\begin{aligned} F_H &= f_H \exp(2\pi i P_H) = C \left[\frac{1}{3} \exp(2\pi i m h_A / d_{111}) \right. \\ &\quad \left. + \frac{2}{3} \exp(2\pi i m h_B / d_{111}) \right] \exp(-2\pi^2 m^2 \langle u^2 \rangle / d_{111}^2). \end{aligned} \quad (3)$$

For the 111 reflection $m=1$ and for the 333 reflection $m=3$. Using the (111) and (333) measured values of P_H and f_H in Table I, the four unknown model parameters are determined. At RT, the Sn atoms have a one up and two down configuration, where $h_A = 2.32(5) \text{ \AA}$ and $h_B = 1.87(5) \text{ \AA}$. The vibrational amplitude for the Sn atoms was determined to be $\langle u^2 \rangle^{1/2} = 0.08(4) \text{ \AA}$, and the Sn random fraction $(1-C)$ for this sample was $0.18(4)$.

Although the T_4 -site assignment is in agreement with the SXRD results, the XSW-measured vertical distribution of Sn atoms is different (see Fig. 2). At RT Bunk *et al.*⁷ determined a single position for the T_4 -site Sn atom and refined the height to be 1.84 \AA above the surface. While their structure at LT has a similar Sn distribution, one up and two down, their model has a smaller vertical separation in height, 0.26 \AA . The model proposed by Avila *et al.* has a comparable

vertical split in height, 0.49 Å, at both RT and LT. However, their distribution showed the opposite asymmetry, two up and one down.¹⁰

The XSW-determined model parameters appear most similar to those by Petaccia and Floreano *et al.*, who made photoelectron-diffraction (PED) measurements on the (3 × 3) phase and used He diffraction to study the effect of temperature on the local structure of Sn.^{25–27} By analyzing PED from the Sn 4*d* core level, they determined bond information between Sn and the neighboring Ge atoms and found a one up and two down Sn distribution, however, the difference in heights was 0.3 Å. Their temperature studies found an order-disorder behavior near T_C . The measured XSW values for coherent position and fraction were found to be the same for the normal (111) reflection at both RT and 115 K, as expected in an order-disorder phase transition. This is also consistent with the thermal energy being comparable or lower than the barrier height for the transition.¹³

In a separate set of XSW measurements²⁸ on the 1/3 ML Sn/Ge(111) system, the sample was annealed to a higher temperature (573 K) and different values for the Fourier coefficients were found. The analysis of this data indicates an additional, third Sn position, corresponding to Sn substituting for Ge in the bottom of the surface bilayer. This particular 30 min, 573 K thermally activated interfacial diffusion led to 20% of the Sn migrating to this site (compared to less than 5% in the 473 K anneal experiment described above).

These results complement STM images that indicate Ge substituting for Sn in the T_4 site.^{14,15}

In conclusion, the measured Sn XSW Fourier coefficients (amplitude and phase) for a selected set of *hkl* Ge Bragg reflections are combined to produce a 3D direct-space image of the Sn atom distribution within the Ge primitive unit cell. For the $\sqrt{3}$ phase at RT, these XSW measurements show that Sn adatoms are at the T_4 site with two-thirds of the Sn at 1.87 Å above the top of the bulklike Ge bilayer and one-third of Sn at 2.32 Å, i.e., one up and two down. The time-averaged Sn distribution, when projected into the (1 × 1) unit cell, shows no significant change when going through the phase transition. This agrees with an order-disorder transition in which Sn atoms are “frozen” in below T_C and undergo correlated fluctuations above T_C , with little time spent in transition between the two heights.^{6,11} The magnitude (0.45 Å) of the Sn vertical separation from the XSW results agrees with the soft phonon model¹¹ at RT, where the Sn atoms undergo a correlated 0.5 Å switching in their vertical positions.

The authors thank P. Baldo and Z. Zhang for technical assistance and M. Asta and T.-L. Lee for helpful discussions. This work was supported by the NSF under Contract Nos. DMR-9973436, DMR-0076097, and CHE-9810378; the State of Illinois under Contract No. IBHE HECA NWU 96 to NU, and the U.S. DOE under Contract Nos. W-31-109-ENG-38 to ANL and DE-FG02-03ER15457 to NU.

*Present address: MHATT-CAT, Advanced Photon Source, Argonne National Laboratory, Argonne, IL 60439.

¹J. S. Pedersen, R. Feidenhans'l, M. Nielsen, F. Grey, and R. L. Johnson, *Surf. Sci.* **189/190**, 1047 (1987).

²M. Göthelid *et al.*, *Surf. Sci.* **271**, L357 (1992).

³J. M. Carpinelli, H. H. Weitering, M. Bartkowiak, R. Stumpf, and E. W. Plummer, *Phys. Rev. Lett.* **79**, 2859 (1997).

⁴R. I. G. Uhrberg and T. Balasubramanian, *Phys. Rev. Lett.* **81**, 2108 (1998).

⁵G. Le Lay *et al.*, *Appl. Surf. Sci.* **123**, 440 (1998).

⁶J. Avila *et al.*, *Phys. Rev. Lett.* **82**, 442 (1999).

⁷O. Bunk *et al.*, *Phys. Rev. Lett.* **83**, 2226 (1999).

⁸J. D. Zhang, Ismail, P. J. Rous, A. P. Baddorf, and E. W. Plummer, *Phys. Rev. B* **60**, 2860 (1999).

⁹T. E. Kidd, T. Miller, M. Y. Chou, and T. C. Chiang, *Phys. Rev. Lett.* **85**, 3684 (2000).

¹⁰J. Avila *et al.*, cond-mat/0104259 (unpublished).

¹¹R. Pérez, J. Ortega, and F. Flores, *Phys. Rev. Lett.* **86**, 4891 (2001).

¹²G. Ballabio *et al.*, *Phys. Rev. Lett.* **89**, 126803 (2002).

¹³L. Petersen, Ismail, and E. W. Plummer, *Prog. Surf. Sci.* **71**, 1 (2002).

¹⁴H. H. Weitering *et al.*, *Science* **285**, 2107 (1999).

¹⁵A. V. Melechko, J. Braun, H. H. Weitering, and E. W. Plummer, *Phys. Rev. Lett.* **83**, 999 (1999).

¹⁶L. Petersen, Ismail, and E. W. Plummer, *Phys. Rev. B* **65**, 020101 (2002).

¹⁷B. W. Batterman, *Phys. Rev. Lett.* **22**, 703 (1969).

¹⁸J. A. Golovchenko, J. R. Patel, D. R. Kaplan, P. L. Cowan, and M. J. Bedzyk, *Phys. Rev. Lett.* **49**, 560 (1982).

¹⁹M. J. Bedzyk and G. Materlik, *Phys. Rev. B* **31**, 4110 (1985).

²⁰M. J. Bedzyk and G. Materlik, *Phys. Rev. B* **32**, 6456 (1985).

²¹N. Hertel, G. Materlik, and J. Zegenhagen, *Z. Phys. B: Condens. Matter* **58**, 199 (1985).

²²P. F. Lyman, D. T. Keane, and M. J. Bedzyk, in *Synchrotron Radiation Instrumentation*, edited by E. Fontes (AIP, New York, 1997), Vol. CP417, p. 10.

²³In general for XSW measurements, $P_H = -P_{\bar{H}}$ and $f_H = f_{\bar{H}}$. For the Ge(111) surface the threefold surface normal axis yields equivalent results for $(hk\bar{l})$, $(\bar{h}kl)$, and $(h\bar{k}l)$.

²⁴This formulation has also been used to generate 1D distribution functions of bulk impurities in mica. See L. Cheng, P. Fenter, M. J. Bedzyk, and N. C. Sturchio, *Phys. Rev. Lett.* **90**, 255503 (2003).

²⁵L. Petaccia *et al.*, *Phys. Rev. B* **64**, 193410 (2001).

²⁶L. Floreano, D. Cvetko, G. Bavdek, M. Benes, and A. Morgante, *Phys. Rev. B* **64**, 075405 (2001).

²⁷L. Petaccia, *Phys. Rev. B* **63**, 115406 (2001).

²⁸J. S. Okasinski, D. A. Walko, C.-Y. Kim, and M. J. Bedzyk (to be published).